Layer-Thickness Dependence of the Compositions in Strained III-V Superlattices by Atom Probe Tomography

B. Knipfer[a], A. Rajeev[a], D. Isheim[d], J.D. Kirch[a], S.E. Babcock[b], T.F. Kuech[c], T. Earles[e], D. Botez[a] and L.J. Mawst[a]

[a] *Department of Electrical and Computer Engineering*
[b] *Department of Material Science and Engineering*
[c] *Department of Chemical and Biological Engineering*
University of Wisconsin-Madison, 1415 Engineering Drive, Madison WI 53706, USA
[d] *Department of Materials Science and Engineering, Northwestern University*
2220 Campus Dr, Evanston, IL 60208, USA
[e] *Intraband LLC, Madison, Wisconsin 53726, USA*

Abstract
In order to conduction-band engineer quantum cascade lasers (QCLs) for emission wavelength, specifically QCLs emitting at 4.6 μm, precise control over layer thicknesses and compositions is required. In this study, Al/Ga incorporation in a strain-balanced InAlAs/InGaAs superlattice (SL) on InP is characterized as a function of layer thickness, keeping the composition constant, using high-angle annular dark-field (HAADF) scanning transmission electron microscopy (STEM) and Atom Probe Tomography (APT). A SL structure was grown on an InP substrate by organometallic vapor phase epitaxy (OMVPE) at a temperature of 605°C and a reactor pressure of 100 torr, with 5 sec interruption time between layers. The full growth thickness obtained from STEM images was used to calibrate the reconstruction of the atom probe data. From the APT results it was found that the Al and Ga incorporation in thin layers (< 2 nm) is significantly lower (down by as much as 10-15% for 1 nm-thick layers) than the targeted composition, which results in a red-shifted emission wavelength when compared to theoretical-model calculations. This result is further shown to be self-consistent at these compositions when compared to a full QCL structure. By introducing an Al overshoot of 5% in the OMVPE gas phase Al/In ratio for the thinnest barrier layers of a full QCL structure, the emission wavelength was reduced from 4.8 μm to 4.6 μm, in accordance with the modeled wavelength for the design target.

Keywords: A1. Atom Probe Tomography; A3. Organometallic Vapor Phase Epitaxy; A3. Superlattice; B3. Quantum Cascade Lasers

Introduction

Mid-infrared emitting QCL devices typically contain active regions composed of 30-50 repetitions of a strained SL motif. This SL motif contains many quantum wells and barriers of varying thicknesses (1-4 nm) and compositions in order to achieve emission through conduction-band engineering. The first experimental demonstration of a QCL was achieved by Faist [1], at cryogenic temperatures. As the technology matured, continuous-wave (CW) operation at room temperature was also achieved. Carrier-leakage suppression is key for reliable, watt-range CW operation, and has been achieved through active-region designs that employ multidimensional conduction-band engineering of strain-balanced SL layers [2,3]. Precise control over the thickness and composition of each quantum well and barrier is required in order to produce the designed

conduction band, maintain a net strain-balanced state, and attain the designed emission wavelength [4,5].

The SL materials comprising the QCL active region are characterized with high-resolution x-ray diffraction (HR-XRD) and HAADF-STEM to determine layer thicknesses and compositions. HR-XRD is employed for measuring average compositions and thicknesses of a periodic structure but determining if a periodic gradient is present at the interfaces is difficult [4]. TEM is commonly used for measuring layer thicknesses, but as it is a 2D projection of the interface, probing the interface and characterizing gradients is challenging. APT allows the analysis of local compositions and structure at interfaces in 3D which is particularly valuable when the results can be structurally correlated with TEM, and, when applicable, HR-XRD.

APT has been previously employed in conjunction with HR-XRD to quantify the composition gradients for SL motifs with constant thickness and composition [6]. TEM has been used to investigate 8 µm-emitting QCL's, grown with SL layers lattice-matched to InP. The thin barriers, composed of $In_xAl_{1-x}As$, were found to be aluminum deficient and were actually quaternaries (InGaAlAs). In order to compensate for this deficiency, overshoots were used based on the measured thickness of the barrier to more accurately grow the targeted compositions [7]. APT has also been previously employed to investigate SL's of relatively thick layers (10-20 nm) of relevance to 8 µm-emitting lattice-matched QCL's where an asymmetric composition was observed when transitioning from InGaAs to InAlAs corresponding with an excess of indium and red-shifted QCL emission wavelength [4].

In this study, aluminum and gallium incorporation in thin SL layers, strained with respect to InP (~0.5%) is characterized using HAADF-STEM and APT as a function of the layer thicknesses while keeping the composition constant. This is carried out for a strain-compensated InGaAs/InAlAs SL with layers of relevance for QCLs designed to emit at 4.6 µm, in order to better understand the compositional structure of the thinnest layers as well as to help clarify the mechanism responsible for the previously observed interfacial compositional grading within a QCL structure.

Materials and Methods

A specific SL structure was grown on a (001) InP substrate by OMVPE in a close-coupled showerhead (3x2") configuration at a temperature of 605°C, a reactor pressure of 100 torr, a 5 sec interruption time between layers, and a susceptor rotation of 100rpm. The V-III precursor ratios, group III partial pressures, and growth rates are shown below in Table 1.

Table 1: V/III ratios and resulting growth rates used to grow the corresponding target composition.

Structure	*Target Composition*	*V/III Ratio*	*Group III Partial Pressure (Torr)*	*Growth Rate (nm/s)*
SL	$In_{0.44}Al_{0.56}As$	370	1.44E-3	0.11
SL	$In_{0.6}Ga_{0.4}As$	406	1.32E-3	0.10
Upper Cladding	$In_{0.52}Al_{0.48}As$	308	1.73E-3	0.13
Lower Cladding	$In_{0.53}Ga_{0.47}As$	476	1.12E-3	0.08
Full Structure Barrier	$In_{0.44}Al_{0.56}As$	373	1.43E-3	0.11
Full Structure Well	$In_{0.57}Ga_{0.43}As$	422	1.27E-3	0.10

The sources used were: trimethylindium (TMIn), trimethylgallium (TMGa), trimethylaluminum (TMAl), phosphine, and arsine. The TMIn concentration was controlled in a feedback loop with an Epison concentration monitor.

The targeted SL layers were 2x(1 nm:$In_{0.44}Al_{0.56}As$/ 1 nm:$In_{0.6}Ga_{0.4}As$); 2x(2 nm:$In_{0.44}Al_{0.56}As$/ 2 nm:$In_{0.6}Ga_{0.4}As$); 2x(3 nm:$In_{0.44}Al_{0.56}As$/ 3nm:$In_{0.6}Ga_{0.4}As$) and 2x(4 nm:$In_{0.44}Al_{0.56}As$/ 4 nm:$In_{0.6}Ga_{0.4}As$) in the growth direction. The SL structure was bound on one side by 50 nm of $In_{0.53}Ga_{0.47}As$ towards the substrate and terminated by 50 nm of $In_{0.52}Al_{0.48}As$ followed by a thin InP capping layer, shown schematically in Fig. 1a.

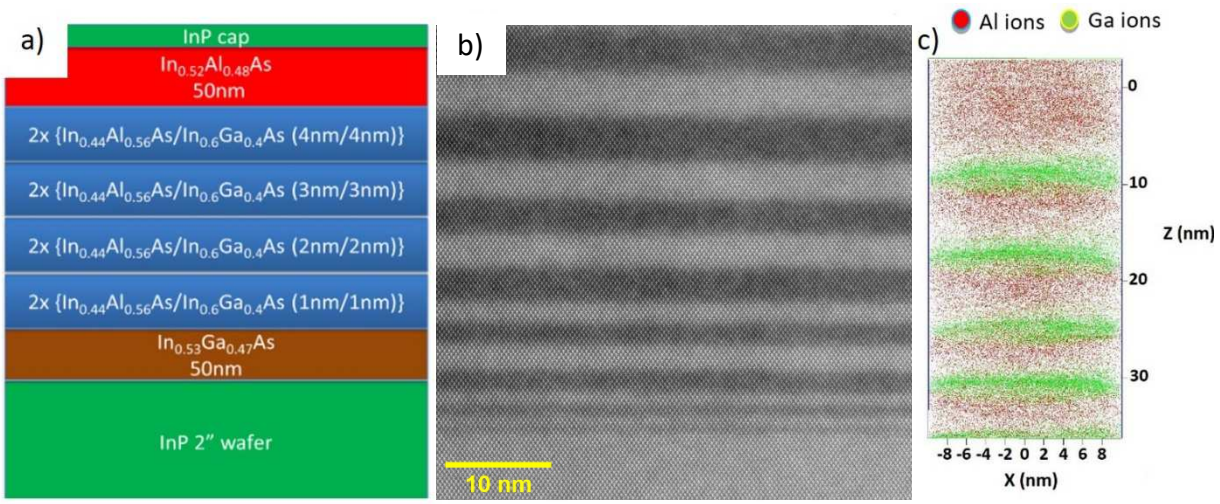

Figure 1: a) Targeted growth for SL structure. b) HAADF-STEM image of the grown SL structure. c) Region of interest analyzed via APT from the SL.

Ga^+ focused ion beam (Ga-FIB) lift out and shaping techniques were used to prepare tips and slices for APT and TEM investigation respectively. The APT tips were shaped with an accelerating voltage of 30kV with progressively smaller radii of annular milling with decreasing current and a Pt protective capping layer (~1um). The final cleaning step was done at 2kV in order to minimize the amount of Ga implantation [8]. The full thickness of the grown layers measured from the HAADF-STEM images was used to calibrate the APT reconstructions to be within 5%. 1-D concentration profiles were obtained in the growth direction from the reconstructions. Atom probe data was collected with a LEAP5000XS with a collection efficiency of 80% at a sample temperature of 30 K in order to maximize spatial resolution in pulsed-laser mode with a repetition rate of 500 kHz, an energy of 1 pJ, and a detection rate of 0.2%. Field evaporation began around 1200 V. A total of three APT tips were run that contained target structures. Two samples contained the structure explained above, the SL, while the third was a full QCL structure. One SL sample ran through the upper few layers but fractured, while the other SL sample began evaporating within the SL and was manually stopped after entering the InP substrate. The third tip, the full QCL structure, began evaporating in the upper $In_{0.53}Ga_{0.47}As$ cladding and continued to evaporate through the following 12 stages of the structure (~600 nm) at which point the tip fractured. While we did not obtain the intended full data set from the 40-stage QCL structure, these data from the first 12 stages do provide results which can be correlated with the SL sample shown in Fig. 1.

All three APT runs were reconstructed in IVAS 3.8.4 using the shank angle model which avoids artifacts from the voltage drops due to the different evaporation fields between the alternating InAlAs/InGaAs layers. Furthermore, to avoid distortions in the peripheral regions of the reconstruction, only the center of each reconstruction is considered for extracting concentration profiles. After identifying suitable isoconcentration surfaces, the Landmark Reconstruction feature in IVAS3.8 was used to ensure planarity and parallelity of the layers in the reconstruction and calibrate the full stage thickness to match that of the HAADF-STEM results, 50.3 nm, for the full QCL structure.

The structure of the full QCL sample is the same as described by Botez [9] with thin barriers and wells at the front of the injector with the target compositions nearly the same as that used in the SL samples. The full QCL structure was investigated in order to ascertain whether significant solid-state diffusion is occurring between the first and last grown stage of the 40-stage structure, about a 5-hour time frame, at an elevated temperature of 605°C. Previous studies observed interfacial mixing in a similar InAlAs/InGaAs SL which was fit to a solid-state diffusion profile allowing for extraction of a diffusion coefficient ($4.1 \times 10^{-23} m^2 s^{-1}$) [6]. Based on this diffusion coefficient, the full 40-stage QCL structure would be expected to exhibit an additional 1.5 nm of interface intermixing between the first stage grown and the last stage grown. Thus, the APT data obtained from such a structure could help elucidate whether solid-state diffusion is one of the primary mechanisms responsible for the observed interfacial compositional profiles.

Results

Volumes from two APT tips from the SL structure shown in Fig. 1a were reconstructed. The reconstruction of the first tip, Fig 1b, had a larger diameter (~20 nm), but fractured before reaching the thin 1nm layers. The second tip, while having a much narrower diameter (~5 nm) and missing the topmost layers of the SL, did include the thin layers and lower cladding. Between these two tips, complete APT data for all the constituent layers of the SL, were obtained. 1-D concentration profiles were obtained in the growth direction from these cylindrical regions of interest, in order to minimize edge-effects and possible Ga implantation from the Ga-FIB. By removing more than 5nm from each side of the tip we should see minimal Ga implantation [8].

Experimental layer thicknesses were approximately 0.9 nm:$In_{0.44}Al_{0.56}As$/1.0 nm:$In_{0.6}Ga_{0.4}As$; 2.0 nm:$In_{0.44}Al_{0.56}As$/ 2.2 nm:$In_{0.6}Ga_{0.4}As$; 3.3 nm:$In_{0.44}Al_{0.56}As$/ 3.3 nm:$In_{0.6}Ga_{0.4}As$ and 4.3 nm:$In_{0.44}Al_{0.56}As$/ 4.1 nm:$In_{0.6}Ga_{0.4}As$ in the growth direction resulting in a total thickness of 42 nm excluding the upper and lower claddings were obtained from HAADF-STEM.

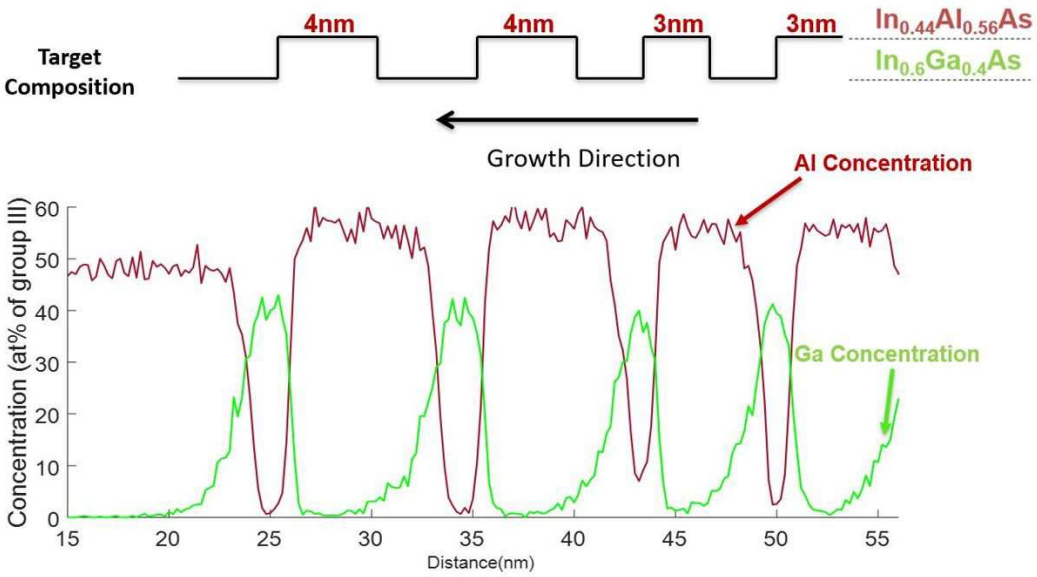

Figure 2: 1D concentration profile of the atomic percent of group III for the first tip through the upper layers of the SL with the targeted thicknesses and compositions above.

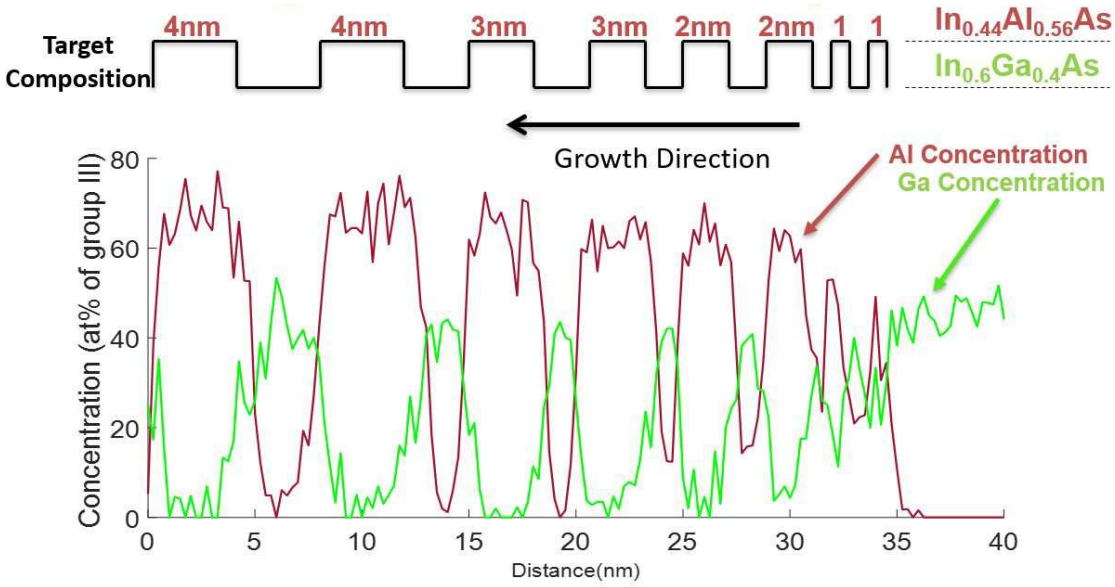

Figure 3: 1D concentration profile of the atomic percent of group III for the second tip from the top of the SL through the thin 1nm layers with the targeted thicknesses and compositions above

The 1D concentration profile of atomic percent group III for the two tips containing the SL are displayed in Figures 2 and 3. The thinner tip has a much narrower tip profile resulting in a noisier concentration profile, shown in Figure 3. There does appear to be an asymmetry in the interfaces, which has been previously observed [4], although we did not observe the corresponding indium segregation. In order to disambiguate potential artifacts of the measurements, the APT analysis of this material would need to be run in the opposite direction, a subject for future studies. Compiling the average composition as a function of the experimentally measured layer thicknesses across both tips is shown in Figure 4. As the layer thickness becomes thinner, the amount of Al or Ga incorporation significantly decreases as well, ~15% deficient at 1nm for Al and ~10% deficient at 1nm for Ga from the respective target compositions.

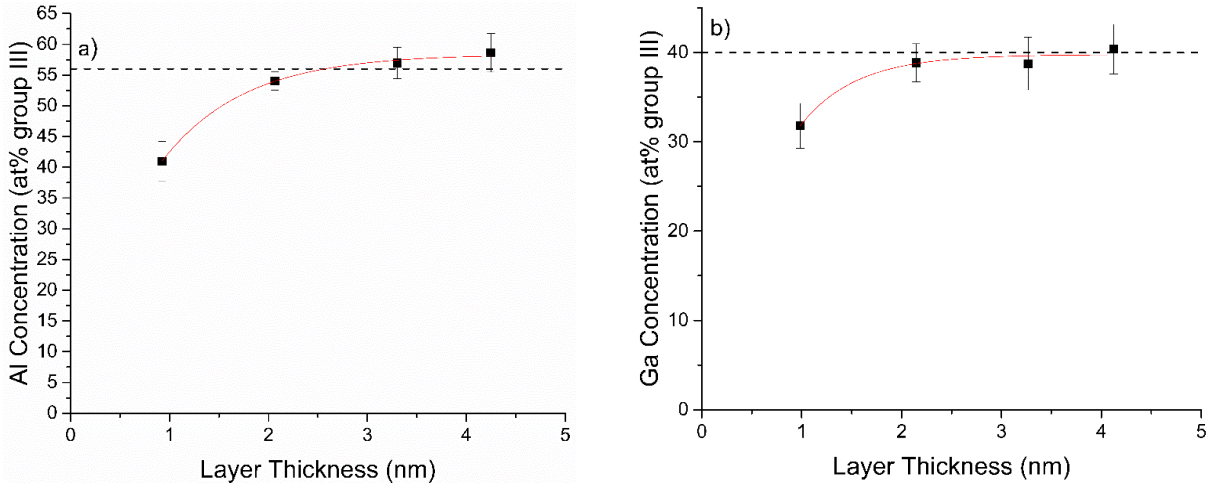

Figure 4: Averaged aluminum (a) and gallium (b) atomic percent of group III as a function of experimentally measured layer thickness. The horizontal corresponds with the targeted composition.

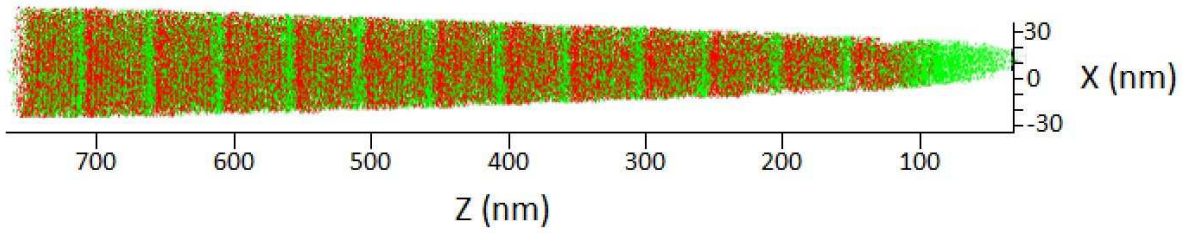

Figure 5: APT reconstruction for the upper 12 stages of the full QCL structure and InGaAs upper waveguide using the Landmark Reconstruction feature in IVAS 3.8.4. The red and green points corresponds with Al and Ga atoms respectively.

As discussed above, quantifying with APT the interfacial compositional grading between the first and the last grown stage for the full QCL structure, and correlating this with a solid-state diffusion model using the extracted diffusion coefficient described by Rajeev [6], would help elucidate whether significant diffusion occurs during the relatively long growth time between active region stages. The tip fabricated from the full QCL (Fig. 5) contains the 1st through the 12th stage, which based on the diffusion model used in [6], would be expected to reveal an intermixing length difference of ~0.3 nm, which is within our error for this measurement. Therefore, from this APT measurement we are unable to make a definitive statement regarding the involvement of solid-state diffusion. However, the thin barriers and wells in the QCL can be compared to the two SL

tips as they have nearly the same target composition and the same growth conditions. The measured compositions track well with the previous results, as shown in Figure 6.

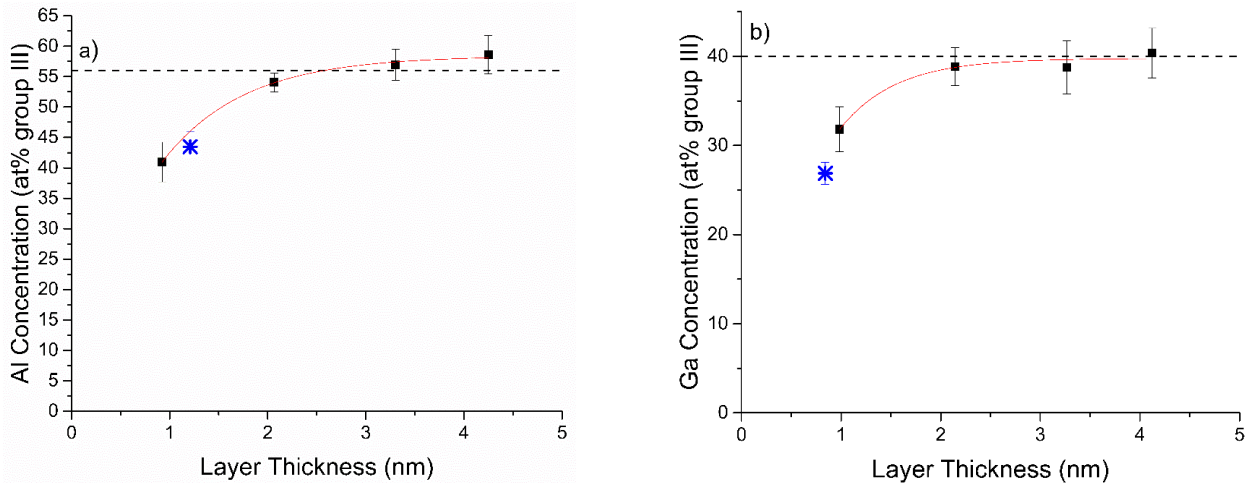

Figure 6: Averaged aluminum (a) and gallium (b) atomic percent of group III incorporated with the additional data point in blue from the full QCL structure with the layer thicknesses measured via HAADF-STEM. Full QCL targets: In0.44Al0.56As/In0.57Ga0.43As.

We previously reported QCLs [10] that emitted at a wavelength (4.8 µm) that was longer than simulated one (i.e., 4.6 µm) using a k*p model and assuming the targeted compositions. APT was performed in order to determine the actual compositions of the thinnest InAlAs barrier layer at the front of injector region of the active stage, as that layer has a large impact on the wavefunctions within the full QCL structure. As can be seen from Figure 6, the amount of Al/Ga incorporated in $In_{0.44}Al_{0.56}As/In_{0.6}Ga_{0.4}As$ has a layer thickness dependence where it is significantly decreased in layers thinner than 2 nm. This decrease in Al has been shown to effectively lower the barrier height, resulting in a longer emission wavelength in QCLs [7]. In order to achieve the modeled QCL emission wavelength, an overshoot for the thinnest InAlAs layer may be necessary [7].

The QCL structure reported in [9] was regrown under the same conditions, except with an overshoot of 5% in the gas phase Al/In ratio in order to increase the Al content in the thinnest injector barrier layer. This resulted in a modeled and experimental wavelength of 4.6 µm. With this overshoot the exact amount of Al incorporated in these layers is unknown, but we can assume it more closely resembles the target composition.

Conclusion

Atom probe tomography has been employed to analyze the layer-thickness dependence of group III incorporation in a strain-balanced SL with relevance to 4.6 µm-emitting QCL's. A lower Al/Ga incorporation (10-15% below target for layer thickness of 1 nm) has been shown via APT measurements in a InAlAs/InGaAs superlattice (SL) with varying layer thickness on an InP substrate. Initial APT studies of a full QCL structure have been performed on the 1st and 12th active-region stage, in order to ascertain whether solid-state diffusion during the long growth is a significant factor in forming the intermixing observed at the interfaces. However, the cause of

intermixing between layers is inconclusive as the amount of diffusion we would expect to observe between the 12 stages of the APT sample obtained is found to be within the error of the measurement. Using an intentional 5% Al flowrate overshoot for the thinnest layers of a QCL, resulted in a convergence of the modeled and experimental wavelengths, further supporting these findings.

[1] J. Faist, et al, Science, Vol. 264, 1994, 553-556. https://doi.org/10.1126/science.264.5158.553.
[2] J. Shin et al, Appl. Phys. Lett., Vol. 94, 2009, 201103. https://doi.org/10.1063/1.3139069
[3] D. Botez et al, IEEE J. Sel. Top. Quantum Electron. Vol. 19, 2013, 1200312. https://doi.org/10.1109/JSTQE.2012.2237387.
[4] C.A. Wang et al, Journal of Crystal Growth, Vol. 464, 2017, 215–220. https://doi.org/10.1016/j.jcrysgro.2016.11.029.
[5] J. Shin et al, Journal of Crystal Growth, Vol. 357, 2012, 15-19. https://doi.org/10.1016/j.jcrysgro.2012.07.013.
[6] A. Rajeev et al, *Crystals* (2018), *8*(11), 437. https://doi.org/10.3390/cryst8110437.
[7] Konstantinos Pantzas et al, Semicond. Sci. Technol. (2016). doi:10.1088/0268-1242/31/5/055017.
[8] K. Thompson et al, Microscopy and Microanalysis, Vol. 12, 2006, 1736. https://doi.org/10.1017/S1431927606065457
[9] D. Botez et al, Opt. Mater. Express 8, 1378-1398 (2018). https://doi.org/10.1364/OME.8.001378.
[10] J. D. Kirch et al, Electron. Lett. Vol. 48, 2012, 234. http://dx.doi.org/10.1049/el.2012.0017.

Acknowledgement: This work is supported by Air Force Research Laboratory under Grant FA8650-13-21616 and NSF ECCS 1806285. Atom-probe tomography was performed at the Northwestern University Center for Atom-Probe Tomography (NUCAPT). The LEAP tomograph at NUCAPT was purchased and upgraded with grants from the NSF-MRI (DMR-0420532) and ONR-DURIP (N00014-0400798, N00014-0610539, N00014-0910781, N00014-1712870) programs. NUCAPT received support from the MRSEC program (NSF DMR-1720139) at the Materials Research Center, the SHyNE Resource (NSF ECCS-1542205), and the Initiative for Sustainability and Energy (ISEN) at Northwestern University. The authors gratefully acknowledge use of facilities and instrumentation at the UW-Madison Wisconsin Centers for Nanoscale Technology partially supported by the NSF through the University of Wisconsin Materials Research Science and Engineering Center (DMR-1720415).